Effect of Ti dopant on the carrier density collapse in colossal magnetoresistance material $La_{0.7}Ca_{0.3}Mn_{1-y}Ti_yO_3$

Xianming Liu,* Xiaojun Xu, and Yuheng Zhang
Structure Research Laboratory, University of Science and Technology of China, Hefei, Anhui 230026, People's Republic of China
(Received 4 January 2000; revised manuscript received 20 July 2000)

The effects of Ti doping on the Mn site in the colossal magnetoresistant (CMR) material of $La_{0.7}Ca_{0.3}MnO_3$ has been studied by preparing the series $La_{0.7}Ca_{0.3}Mn_{1-y}Ti_yO_3$ ($y=0$, 0.01, 0.03, 0.05, 0.07, 0.1, 0.2, 0.3). The Ti^{4+} doping separates the system into ferromagnetic (FM) clusters, and the spin coupling between these FM clusters is weakened with increasing doping content. These variations lead to the decrease of the magnetization M and widening of the paramagnetic-ferromagnetic (PM-FM) transition. When $y \geqslant 0.1$, the size of the FM clusters is so small that there is nearly no interaction between these clusters. The PM-FM transition transforms to paramagnetic–spin-glass transition gradually because the cluster spin arranges randomly. Because the substitution of Ti^{4+} depletes the oxygen p holes and leads to the increase of the bipolaron binding energy, the collapse of the unbound polaron density is reduced. Therefore, the resistivity ρ increases, and the temperature T_ρ corresponding to the resistivity maximum ρ_{max} shifts to a low temperature with the doping content. For heavy doping, the samples exhibit an insulating behavior in the entire temperature range studied. Moreover, the substitution of the Ti^{4+} ions extremely enhances the CMR effect in the perovskite manganite materials.

I. INTRODUCTION

Over the past years, the doped $LaMnO_3$ system is the one of the most interesting topics due to its unusual magnetic and transport properties, especially the colossal magnetoresistance (CMR) phenomena.[1–4] The parent compound $LaMnO_3$ is an antiferromagnetic insulator. It exhibits both ferromagnetism and metallic conductivity at a low temperature when La^{3+} ions are partially substituted with 2+ valence ions such as Ca, Sr, Ba, Pb, and Cd. This property was explained within the framework of the double exchange (DE) interaction by Zener, which results in a varying bandwidth of holes doped into the Mn^{3+} level.[5–7] But it is not sufficient to explain all the physics in these materials alone. It has been claimed that an additional electron-phonon coupling that is strong enough to ''self-trap'' the conduction electrons at high temperatures must be required.[8–12] The strong coupling is due to the fact that in its d^4 configuration, Mn^{3+} is a Jahn-Teller (J-T) ion. The local J-T distortion of the Mn-O octahedron lowers the energy of the e_g electron of the Mn 3d level. As a result, the charge carriers can be localized to form lattice polarons when the bare bandwidth is narrow enough. A series of experiments, such as transport measurements,[13–15] spectroscopy analysis,[16–18] isotopic effect,[19] and inner friction[20] provides evidences for the polaron transport in the perovskite manganites. Within these DE and polaron models, scientists have studied the electronic, magnetic, and optical properties in wide-field, temperature, pressure, doping, and post-treating ranges.

However, some experimental results showed that the idea of a ''metallization'' of manganites is not tenable and the polaronic hopping is also the dominant conduction mechanism below the Curie temperature T_C.[21–25] The doped manganites are charge-transfer-type oxides with carriers having significant oxygen 2p hole character. The holes are coupled antiferromagnetically with the d^4 local moments of the Mn^{3+} ions and become itinerant, thus aligning the Mn moments ferromagnetically.[21,26] The role of the oxygen hole density must be considered to satisfactorily describe charge carrier transport properties. Recently, we mentioned that Alexandrov and Bratkovsky proposed a theory[27] of the ferromagnetic/paramagnetic (FM/PM) phase transition in doped charge-transfer magnetic insulators accompanied by a charge carrier density collapse (CCDC) and CMR. It is based on the fact that the doped manganites have oxygen p holes as the charge carriers rather than d (Mn^{3+}) electrons. They found a novel ferromagnetic transition driven by nondegenerate polarons, explaining a tendency of polarons to form bound pairs and the (competing with binding) exchange interaction of p polaronic holes with d electrons. There is a sharp increase of the polaron density at temperatures below a critical temperature T_C'. The charge carrier density collapse results in unusual behavior of CMR materials and a huge sensitivity of the carrier transport to the external field.

Despite the exhaustive study of the effects of the rare-earth doping in these manganites, the influence of the substitution at Mn sites with other elements has attracted much more attention. Previous works[28–32] show that the trivalent and tetravalent elements substitution for Mn sites strongly affects the electronic transport and magnetic behaviors. Maignan *et al.*[32] indicate that whatever the element, the transition temperature separating the ferromagnetic metallic state and the paramagnetic insulating state decreases dramatically when the substituted element content is increased, the saturated magnetic moment at low temperature being slightly decreased. Furthermore, the substitution on Mn sites can result in the CMR effect several times larger than pristine manganite. They also find that all the doping elements exhibit a d^0 or d^{10} electronic configuration. It results in the absence of unpaired electrons on the doped Mn sites, which may break the hole propagation in the manganese-oxygen lattice, as the doping content increases, and consequently leads to a de-

crease of T_C. The small difference between the different substitutions would then just be due to the combined effects of the size and of the valence of the dopants. We conceive that the trivalent and tetravalent elements substituted would occupy the Mn(III) and Mn(IV) sites, respectively, and the doping on Mn sites with unchangeable tetravalent element inevitably weaken the DE interaction in Mn^{3+}-O-Mn^{4+} covalent structures. It is expected that the electrical and magnetic properties and the CMR effect will be more sensitive to the substitution of the tetravalent element. But, first we must demonstrate that the tetravalent element just only occupies the Mn(IV) site. In this paper, we have chosen the Ti^{4+} ion as a substitute for the Mn ion because it has no 3d shell and $CaTiO_3$ is a well-known perovskite. Although the results of $\rho \sim T$, $M \sim T$, and CMR are consistent with previous reports,[32] in our work the infrared transmission spectra demonstrate not only the occupation of Ti^{4+} on the Mn(IV) sites but also no observable change in the Jahn-Teller distortion of MnO_6 octahedra. Our experiment finds that there exists the transition from paramagnetic to cluster-spin glass (CSG) states. Due to the existence of the CSG state, both the electrical and magnetic properties are dramatically changed with the Ti doping. We also fitted the resistivity with the CCDC model; a better understanding of the physical mechanism can be obtained based on the CCDC theory.

II. EXPERIMENT

Polycrystalline $La_{0.7}Ca_{0.3}Mn_{1-y}Ti_yO_3$ ($y=0.0$, 0.01, 0.03, 0.05, 0.07, 0.1, 0.2, 0.3) samples were fabricated with the conventional solid-state reaction method. The powder of La_2O_3, $CaCO_3$, $MnCO_3$, and TiO_2 with different stoichometries was mixed and heated in air at 1250 °C for 20 h. Then they were ground heavily and fired in air at 1250 °C for 20 h again. After grinding they were pressed into pellets and sintered in air at 1350 °C for 25 h. X-ray powder diffraction patterns were collected at room temperature using a D-Max Rigaku system with a rotating anode of Cu. Magnetic measurements were carried out by using a commercial vibrational sample magnetometer. The resistivity measurements with and without magnetic field were performed by a standard four-probe method. A superconducting coil was used to produce steady magnetic fields. The micromagnetic property of the samples has been investigated by the measurements of electronic spin resonance (ESR) spectra. The frequency of the microwave used in the measurements is 9.46 GHz and the limit of the lowest temperature in the ESR experiments was 100 K.

III. RESULTS AND DISCUSSION

A. Substitution of Ti for the Mn site

X-ray diffraction patterns of the samples of the $La_{0.7}Ca_{0.3}Mn_{1-y}Ti_yO_3$ ($y=0.0$, 0.01, 0.03, 0.05, 0.07, 0.1, 0.2, 0.3) are presented in Fig. 1 showing clean single-phase patterns for all samples. For the sample with $y=0$, the crystal structure is cubic, which agrees with an early report.[33] With the increase of y concentration, no orthorhombic line splitting was observed. Although the crystal structures of these samples do not change with the Ti doping, the lattice parameter increases from $a_0=0.383$ nm for $y=0$ to $a_0=0.389$ nm for $y=0.3$, indicating that the partial Mn sites were occupied by the Ti^{4+} ions because the Ti^{4+} ion radius (0.0605 nm) is larger than the Mn^{3+} one (0.053 nm).[34] Upon the Ti doping, the tolerance factor defined by Goldschmidt $t=(r_A+r_O)/2^{1/2}(r_B+r_O)$ varies slightly from $t=0.979$ to $t=0.968$. In fact, the perovskite structure is stable for $0.89<t<1.02$. Therefore, the substitution of Ti does not affect the crystal structure of these samples, except for a slight increase of the lattice parameter.

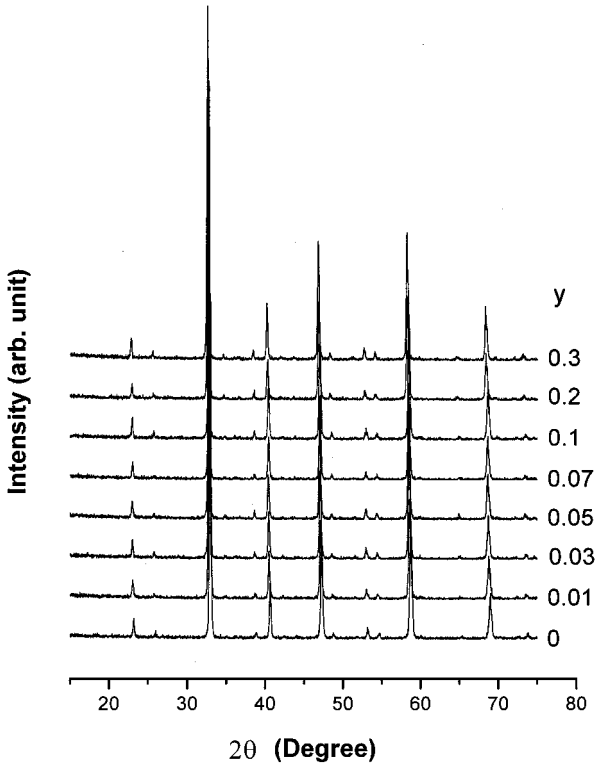

FIG. 1. X-ray diffraction pattern of $La_{0.7}Ca_{0.3}Mn_{1-y}Ti_yO_3$ samples. All the samples are cubic.

In order to demonstrate the substitution of Ti for an Mn ion in a tetravalent ion, and to check the influence of Ti doping on the J-T distortion, the samples were measured by the infrared (IR) transmission spectrometer. Figure 2 gives the IR transmission spectra of the $La_{0.7}Ca_{0.3}Mn_{1-y}Ti_yO_3$ samples with different Ti content. The two strong absorption peaks located at $\nu_3 \approx 590\,cm^{-1}$ and $\nu_4 \approx 393\,cm^{-1}$ may be attributed to the internal phonon modes, stretching ν_3 and bending ν_4,[35] of MnO_6 octahedra. The internal phonon modes can reflect J-T distortion, due to the fact that the J-T distortion only occurs in the MnO_6 octahedra. As the Ti content increases, the shift of these two peaks was not evident. This indicates that the J-T distortion, therefore the MnO_6 octahedra, had no noticeable change upon the replacement of Mn by Ti. Otherwise, there are remarkable differences in the features of the IR spectra among these samples. The absorption peak of the stretching mode ν_3 widened and became asymmetric gradually with the doping level. For $y=0$, there were two transmission peaks that appeared at the two sides of the stretching mode ν_3 symmetrically. With the increase of the doping content y, the transmission peak at low frequency decreases while the one with high frequency shifts to

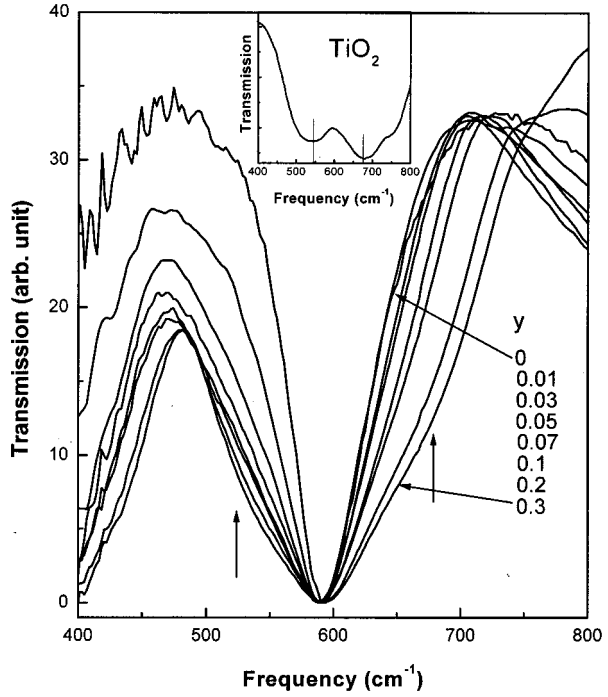

FIG. 2. Infrared transmittance spectra taken in the frequency range of 350–4000 cm^{-1} for $La_{0.7}Ca_{0.3}Mn_{1-y}Ti_yO_3$ samples.

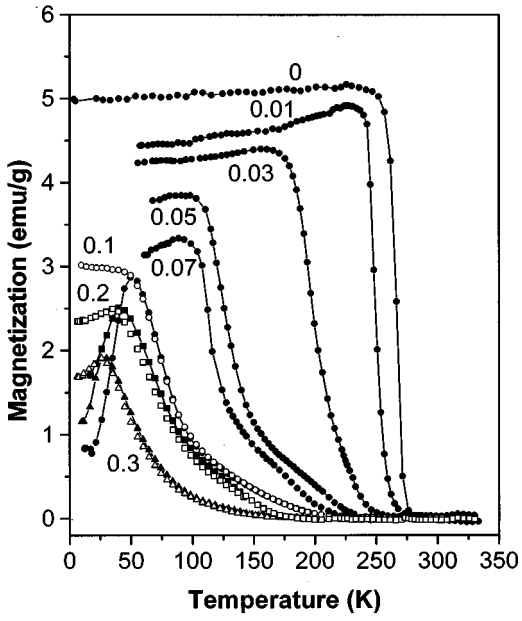

FIG. 3. Temperature dependence of the magnetization M in a 50-G field for $La_{0.7}Ca_{0.3}Mn_{1-y}Ti_yO_3$ samples.

higher frequency. The two shoulders grew on the two sides of the stretching peak for heavy doping samples.

The widening of the stretching peak may be induced by the following two vibrations: (i) the Mn-O stretching vibration in the Mn-O-Ti structure and (ii) the Ti-O stretching vibration in TiO_6 octahedra. In order to determine the influence of Ti doping on the IR transmission spectrum, we have shown the IR spectrum of pure TiO_2 in the inset of Fig. 2. There are two absorption peaks at 670 and 540 cm^{-1}, respectively. The positions of the two shoulders in Fig. 2 are just about 672 and 540 cm^{-1}. By comparing the spectra with the spectrum of pure TiO_2, it can be found that the two weak shoulders can be attributed to the Ti^{4+}-O^{2-} bond. From the results above, we suggest that the Ti occupies the Mn sites in the form of the tetravalent ion. This is consistent with previous work.[32,36] Due to the electronic configuration, the Ti^{4+} doping for Mn ions would affect strongly the electrical and magnetic properties of this material.

B. Magnetic property

Paramagnetic to clusterlike spin-glass phase transition

The temperature dependence of the magnetization M for the Ti-doped samples $La_{0.7}Ca_{0.3}Mn_{1-y}Ti_yO_3$ is shown in Fig. 3. The magnetization M was measured at the magnetic field of $\mu_0 H = 50$ G in the warming process with the samples zero field cooled (solid symbol curves). The temperature T_C of the PM-FM transition is listed in Table I, where the T_C is defined as the temperature corresponding to the peak of dM/dT in the M vs T curve. The table shows that the PM-FM transition temperature T_C shifts to a lower temperature upon the Ti doping. The undoped sample undergoes a PM-FM transition at the temperature $T_C = 267$ K because the coupling of the oxygen p holes with the d^4 local moments on Mn^{3+} ions aligns the moments ferromagnetically.[27] With increasing the Ti doping level, the magnetization M is suppressed and the PM-FM transition is obviously broadened for $y \geqslant 0.03$ (see Fig. 3). The significant suppression of the magnetization M and the large decrease of the PM-FM transition temperature T_C suggest that the Ti doping strongly weakens the exchange interaction between the p holes and 3d electrons, which is the origin of the ferromagnetism in these manganites according to the CCDC model.

The transition broadening was also observed in the perovskite materials substituted by the trivalent ions for Mn sites,[13,29,30] and is more sensitive to the substitution of the tetravalent ion, as we observed. In the Ti-doped samples, because the electron configuration of the Ti^{4+} ion is $3p^6 3d^0$, there is no exchange interaction of p holes with the 3d electrons in the O^{2-} L–Ti^{4+} (L is a 2p hole in oxygen) groups, i.e., $J_{pd} = 0$. The moments of the Mn^{3+}-O^{2-}-Ti^{4+} covalent

TABLE I. Electronic transport and magnetic properties of $La_{0.7}Ca_{0.3}Mn_{1-y}Ti_yO_3$ samples. T_C is the temperature of ferromagnetic-paramagnetic transition as determined from magnetization measurements. T_ρ is the temperature corresponding to the resistivity maximum for $H = 0$ T. T_m is the temperature corresponding to the MR peak for $H = 3$ T. $[\Delta\rho/\rho_H]_m$ is the peak value of MR at $T = T_m$ for $H = 3$ T. T_P and T_F are the temperatures corresponding to the paramagnetic peak and the ferromagnetic peak beginning to disappear and appear measured from PER spectra, respectively.

Composition	0	0.01	0.03	0.05	0.07	0.1	0.2	0.3
T_C (K)	267	248	196	123	112	71	65	42
T_ρ (K)	273	253	211	153	113			
T_m (K)	270	246	199	140	109	63		
$[\Delta\rho/\rho_H]_m$ (%)	150	200	220	570	1550	4750		
T_P	250	245	200	110	<100	<100	<100	<100
T_F	259	265	245	245	230	220	200	170

structures cannot be aligned ferromagnetically. Furthermore, the doping of Ti^{4+} ions causes the inhomogeneous distribution of the $Mn^{3+}-O^{2-}L-Mn^{3+}$ covalent structures in the samples and disrupts the long-range ferromagnetic order between the Mn^{3+} ions. This results in the short-range ferromagnetic clusters with different sizes distributed randomly in the samples. The ferromagnetic cluster with different sizes has different PM-FM transition temperature T_C, therefore, widening the PM-FM transition and decreasing the T_C. This T_C is not the result of the long-range ferromagnetic ordering, but the collective contribution of the clusters all being short-range ferromagnetic ordering.

It is also observed that the magnetization M increases smoothly with decreasing temperature before reaching the maximum value, and it attenuates very rapidly after this maximum point to form a cusp at around 50 K for Ti content $y \geqslant 0.1$. Therefore, we measured the M-T curves for the samples $y \geqslant 0.1$ field cooled, shown in Fig. 3 by an open symbol line. There exists an obvious ''λ'' transition in the M-T curves for the samples field cooled and zero field cooled. This result may imply the existence of clusterlike spin glass (SG) in the ferromagnetic phase at low temperature.[29] The Ti^{4+} doping induces the formation of the FM clusters in the samples, and the distance between the $Mn^{3+}-O^{2-}L-Mn^{3+}$ clusters increases with the doping content. There is no interaction between these clusters for the heavily doped samples $y \geqslant 0.1$. For the samples $y \geqslant 0.1$ zero field cooled, each of the clusters undertakes a transition from paramagnetic to ferromagnetic phase and this transition only occurs in the inside of the clusters. Although all the clusters are ferromagnetic individually, the magnetic moment of each cluster arranges randomly. When the sample is cooled under zero magnetic field, the moments of these ferromagnetic clusters are frozen to low temperature, so that the whole system is in the spin-glass state. The appearance of the spin-glass state induces the decrease of the magnetization at lower temperature. By cooling the samples under a magnetic field, the cluster moments arrange more ordering than that for cooling with zero field, which causes an increase of the magnetization. So the obvious ''λ'' transition appearing in the M-T curves for the samples $y \geqslant 0.1$ represents the paramagnetic–spin-glass transition.

From the above discussion, we obtain the following. The primary material $La_{0.7}Ca_{0.3}MnO_3$ is entirely ferromagnetic at low temperature. As the temperature decreases the PM-FM transition happens in a very narrow temperature range. With the Ti doping, the PM-FM transition is broadened and the magnetization is suppressed. Even more, there exists clusterlike spin-glass phase at low temperature for heavily doped samples. In order to demonstrate the conclusions for the variation of the macroscopic magnetic properties, the microscopic magnetic characters have been studied by ESR. The ESR spectra taken at different temperatures are shown in Fig. 4. In these spectra, only a typical PM peak with the Landé factor $g \approx 2$ is observed at the temperature $T > T_C$ for the undoped sample $y = 0$. There is still a single peak in the spectrum for the sample cooled to 260 K. When the temperature decreases to 258 K, an obvious FM peak grows in the region of low magnetic field, despite the existence of this PM peak. At temperature $T = 250$ K, the PM signal disappears completely and only the FM peak exists in the spectrum.

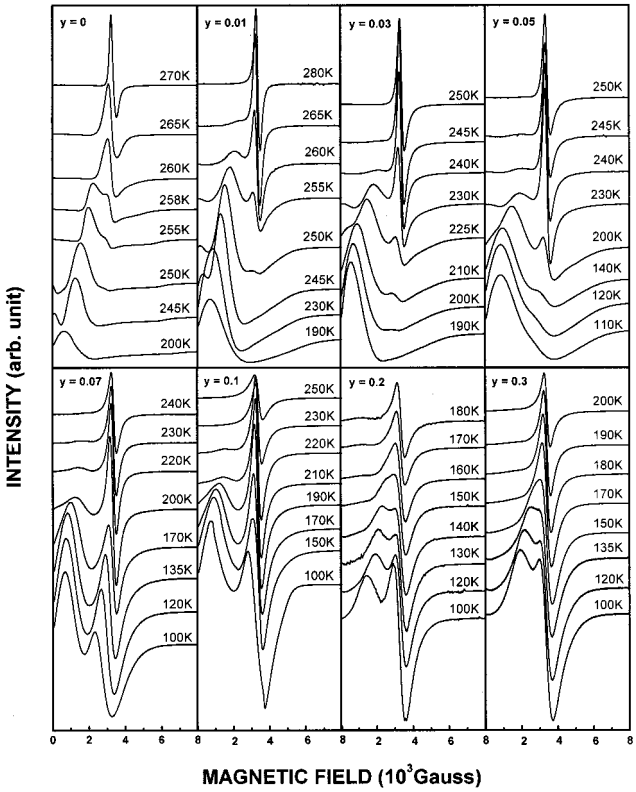

FIG. 4. Electronic spin resonance spectra of $La_{0.7}Ca_{0.3}Mn_{1-y}Ti_yO_3$ samples at different temperatures with the wicrowave frequency $f = 9.46$ MHz.

This transition is only in the 10-K range. From the M-T curve of $y = 0$ sample shown in Fig. 3, we note that the PM-FM transition just occurs in this region. For the samples $y \neq 0$, the FM state appears at a temperature much higher than T_C. As the doping level is higher than 0.07, we can see that the PM and FM peaks exist simultaneously in the ESR spectra in the temperature range of 100 to T_C.

We denote T_P and T_F as the offset temperature of the paramagnetic peak disappearing and the onset temperature of the ferromagnetic peak beginning to appear, respectively, listed in Table I. The data show that both the T_P and T_F shift to lower temperature and the difference ΔT of T_P and T_F increases with the doping content y. In the coexistence regime of the two magnetic phases, the intensity ratio of the paramagnetic to ferromagnetic peak increases with the Ti concentration at the same temperature. These results are consistent with the suppression of the magnetization and the broadening of the PM-FM transition observed in the magnetization measurements and can be explained under the assumption that the samples are magnetically inhomogeneous, as described above. The source of this magnetic disorder is the presence of Ti in the Mn sublattice, separating the system into clusters.

C. Electrical property

Reducing of charge carrier collapse induced by Ti doping

The dramatic change of the magnetic behavior is tightly related to the electrical property of the Ti-doped samples. Figure 5 shows the zero-field resistivity ρ versus temperature

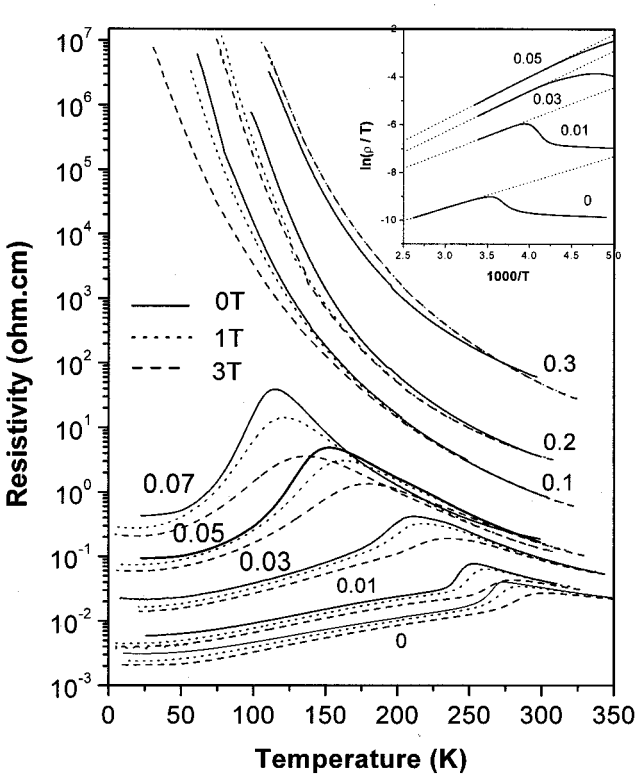

FIG. 5. Electric resistivity ρ in zero (solid line), 1 T (dotted line), and 3 T (dashed line) magnetic field, for $La_{0.7}Ca_{0.3}Mn_{1-y}Ti_yO_3$ samples.

for the samples with different doping level y. The resistivity for all samples increases in the whole temperature range when the Ti content is increased. In the range of $0 \leqslant y \leqslant 0.07$, a resistivity maximum $\rho_{\max}$ is observed at the temperature T_ρ. Furthermore, the magnitude of $\rho_{\max}$ increases and the peak shifts to lower temperatures with increasing the doping level. These results are consistent with ones for Pr-based manganite doped by Ti.[32] At a higher temperature than T_ρ the $\ln(\rho/T) \sim 1000/T$ curves (as shown in the inset of Fig. 5) follow linear correlation for light doped samples, which indicates the transport mechanism of the polaron hoping. For higher content ($y \geqslant 0.1$) the resistivity curves exhibit an insulating behavior in the entire studied temperature range. The experimental setup limits the resistivity measurements to around $10^6\ \Omega$ cm for the samples. Nevertheless, even at low temperature (5 K) no measurable resistivity was obtained for these samples. As shown in Table I, both T_ρ and T_C decrease with increasing y content and T_ρ is always higher than the respective T_C for each sample. In Fig. 5, we have also shown the resistivity $\rho(H, T)$ in an applied magnetic field of $\mu_0 H = 1$ and 3 T. With the exception of the doping concentration $y = 0.3$, the suppression of ρ in the magnetic field persists over the entire temperature range although the effect decreases above T_C. For each sample of doping concentration $y < 0.1$, T_ρ shifts to a higher temperature with the intensity of the applied magnetic field.

In the CCDC model,[27] it is the localization of p holes into immobile singlet or triplet bipolarons combined with their exchange interaction with the Mn d^4 local moments that are responsible for CMR. The strong electron-phonon interaction is so strong that the bipolarons are really immobile in cubic manganites. Only the single (unbound) hole polarons are the charge carriers, even at low temperature. There is a collapse of the single polaron density at a critical temperature T_C'. The physical origin of the unusual collapse lies in the instability of the bipolarons below T_C' due to the exchange interaction of the polarons with d electrons. The density (n) of single (unbound) hole polarons and the magnetization (σ) of Mn^{3+} ions can be obtained by the following equations.[27]

$$n = 2vy \cosh[(\sigma + h)/t], \tag{1}$$

$$m = n \tanh[(\sigma + h)/t], \tag{2}$$

$$\sigma = B_2[(m + 4h)/t], \tag{3}$$

$$y^2 = (x - n)/(2v^2)\exp(-2\delta/t). \tag{4}$$

Here, m is the absolute value of the magnetization of holes. The dimensionless temperature $t = 2k_BT/J_{pd}S$, magnetic field $h = 2\mu_B H/J_{pd}S$, and the binding energy $\delta \equiv \Delta/J_{pd}S$, in which Δ is the bipolaron binding energy and $J_{pd}S$ is the exchange interaction of p holes with four d electrons of the Mn^{3+} ion, $B_s(x) = (1 + 1/2S)\coth[(S + \frac{1}{2})x] - (1/2S)\coth(x/2)$ is the Brillouin function, while S ($=2$) is the Mn^{3+} spin and v ($=3$) is the degeneracy of the p band.

When the sample is cooled down through the critical point T_C', the bipolarons are broken apart by the exchange interaction of the polaron with the d electrons, resulting in a sharp peak of carrier density. It is assumed that the exchange between the spins on Mn and triplet state bipolaron is suppressed because these bipolarons are strongly more localized. The triplet bipolarons, if they were formed in the paramagnetic phase, can survive in the ferromagnetic phase, thus reducing the carrier density collapse. Therefore, its contribution must be subtracted from the carrier density deduced from Eq. (1):

$$n = n_0/[1 + a\sigma \exp(T/b)], \tag{5}$$

where a and b are adjustable constants, n_0 is the density of unbound single polarons determined by Eq. (1), including the polarons released from the singlet and triplet bipolarons, and σ is the normalized magnetization determined by Eq. (3).

Figure 6 shows the comparison of the experimental resistivity data with the fitting results by the above equations for the samples of $y \leqslant 0.1$. In this fitting process, we use the experimental magnetization data as σ, i.e., $\sigma = M/M_{\max}$. It can be found that there is a very abrupt increase of the carrier density n_0 at the critical temperature T_C' when temperature is cooled down. The fitting results are poorly consistent with the resistivity curves at the temperature $T < T_C'$ because the density n_0 includes the polarons broken apart from the triplet bipolarons. After rectifying for the triplet bipolarons, the theoretical line is fairly consistent with the experimental data. From the fitting results, we obtained the binding energy of the bipolaron and the exchange interaction between the p holes and d electrons, listed in Table II. It is found that the binding energy of the bipolaron Δ and the dimensionless binding energy δ increase with the Ti concentration. It is usually the case that the triplet states always lie higher in energy than the singlet states. We consider that the probabil-

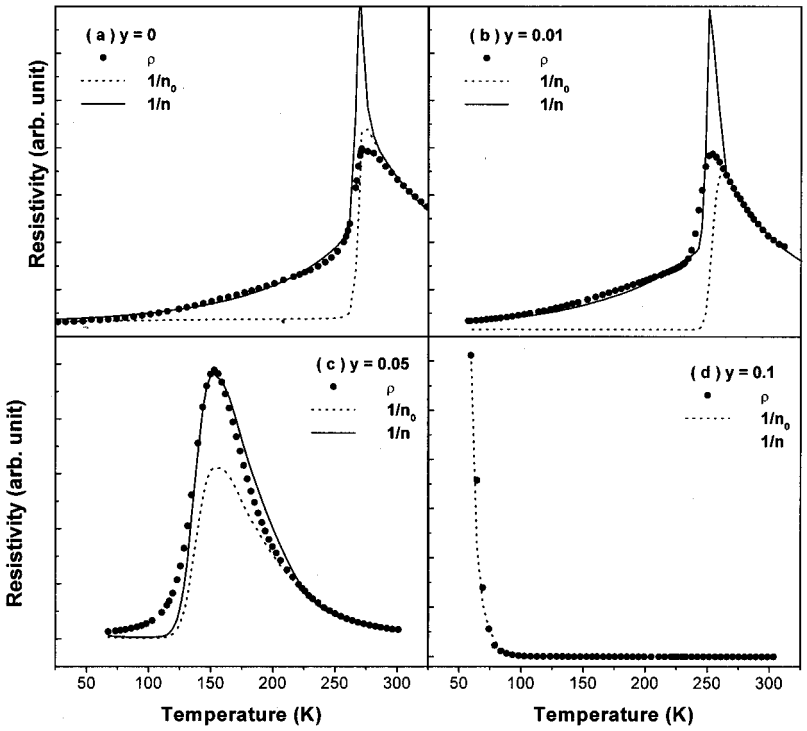

FIG. 6. Comparison of the experimental data of the resistivity with the fitting result and the rectified result by using the CCDC theory for $La_{0.7}Ca_{0.3}Mn_{1-y}Ti_yO_3$ samples.

ity for the formation of a triplet bipolaron should be inversely proportion to the doping concentration. The fact that the bipolaron binding energy Δ increases with the Ti doping implies the increase of the triplet bipolaron number. The carrier density will decrease; then the resistivity increases, with the Ti doping because the triplet bipolarons can survive in the lower temperature. For the sample of $y=0.1$, $\delta=3.5$, the exchange interaction J_{pd} decreases very quickly from 2600 to 1000 K. Because of the competition between the bipolaron binding energy with the exchange interaction, the bipolarons cannot be broken apart, neither triplet nor singlet. When $y=0.3$, there are no p holes doped into the manganite. The samples of $y \geqslant 0.1$ show an insulative behavior.

D. Large enhancement of the CMR effect

The MR ratio is plotted in Fig. 7 as a function of temperature for the samples $y \leqslant 0.1$ under various magnetic fields. It is defined as $\Delta\rho/\rho_H=(\rho_0-\rho_H)/\rho_H$, where ρ_0 is the zero-field resistivity and ρ_H is that under a magnetic field H. The MR ratio displays a maximum at the temperature T_m slightly lower than T_ρ. It is found that with increasing the magnetic field the MR peak moves closer to temperature T_ρ for $\rho_{\max}$ in zero field and the maximum value of the MR ratio increases and shifts to lower temperatures with increasing the doping level y ($y \leqslant 0.1$). The MR ratio increases from 70 for $y=0$ to

TABLE II. Bipolaron binding energy and exchange interaction between p holes and $3d$ electrons, which are obtained by fitting the experimental data of resistivity using the CCDC theory.

Ti content	0	0.03	0.05	0.1
Δ (K)	1950	2550	2850	3500
$J_{pd}S$ (K)	2200	2600	2600	1000
δ	0.886	0.981	1.096	3.500

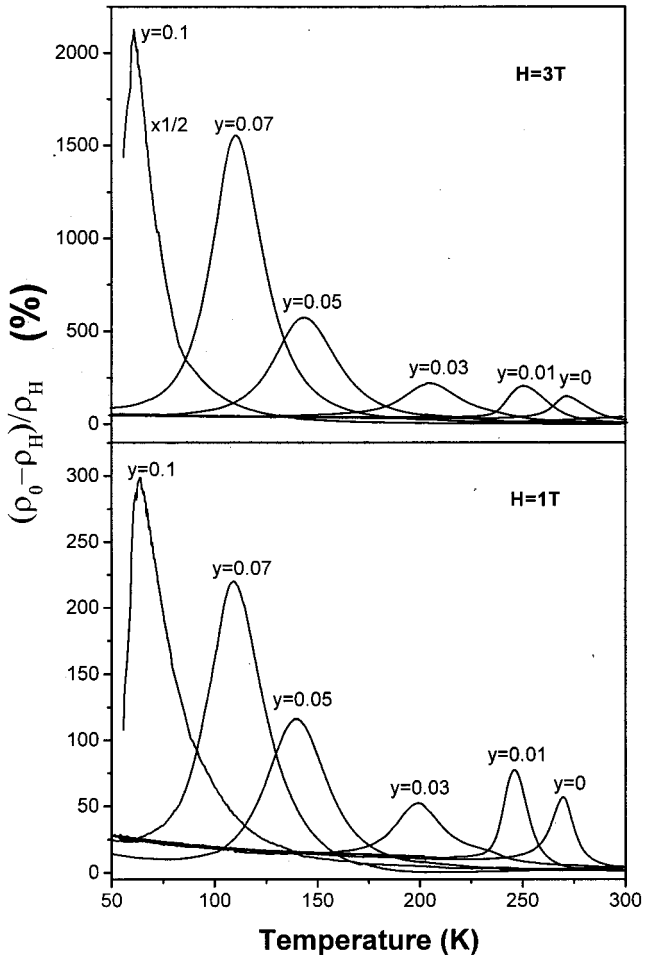

FIG. 7. Temperature dependence of magnetoresistance for $La_{0.7}Ca_{0.3}Mn_{1-y}Ti_yO_3$ samples in a magnetic field $H=1$ T (lower panel) and 3 T (upper panel).

280 for $y=0.1$ at a magnetic field of $H=1$ T, and from 150 for $y=0$ to 4750 for $y=0.1$ under the field of $H=3$ T. However, negligible MR or very small positive MR is observed for the doping concentration of $y=0.2$ and 0.3, respectively. The enhancement of the CMR effect is similar to the previous report by Maignan, Martin, and Raveau.[32]

The Ti doping caused a decrease of the doping concentration in a form of $x=0.3-y$. This decrease is different from directly reducing the Ca^{2+} doping. For example, in $La_{1-x}Ca_xMn_{1-y}Ti_yO_3$ material, the resistivity for $x=0.3$, $y=0.05$ as we observed is larger than that for $x=0.25$, $y=0$ observed in the experiment.[37] Based on the magnetic and electric properties of the $La_{0.7}Ca_{0.3}Mn_{1-y}Ti_yO_3$ material, we believed that the Ti^{4+} substitution not only reduces the hole density, but also enhances the localization of p holes due to a random field. However, an external magnetic field will make the p polaronic holes delocalize, thus breaking apart the bipolarons. The CCDC model shows that the carrier density n and magnetization σ are magnetic field dependent; CCDC has an important role in the CMR effect. Our results show that the CMR effect is extremely enhanced by the Ti^{4+} doping for $y\leqslant 0.1$. After doping, the Ti^{4+} ions separate the system into clusters because there is no exchange interaction between the p holes and Ti^{4+} ions that has no $3d$ electrons, and the PM-FM transition can occur in these clusters. The long-range ferromagnetic order transits gradually into the short-range ordering in the clusters with the doping content. The more the doping content, the smaller will be the size of the clusters. The moments of these clusters arrange randomly. This means that the coupling between the ferromagnetic spins of the clusters is weakened with the Ti doping. Therefore, it is easier to form the short-range FM ordering and to align the moments of the clusters under an applied magnetic field. This will result in the increase of the magnetization and more bipolarons will be broken apart. The FM transition in these clusters leads to the decrease of the resistivity and increase of the CMR effect under the applied magnetic field. From the above results, we can conclude that the Ti^{4+} doping extremely enhances the CMR effect.

IV. SUMMARY

In summary, we have studied the effects of Ti doping in $La_{0.7}Ca_{0.3}MnO_3$ material. As the doping content y increases, the magnetization M is suppressed and the PM-FM transition is broadened. The Ti^{4+} doping separates the system into the ferromagnetic clusters. The spin coupling between these FM clusters is weakened with doping content, which leads to the decrease of the magnetization M and widening of the PM-FM transition. For $y\geqslant 0.1$, the size of the FM clusters is so small that there is nearly no interaction between these clusters. The cluster spins arrange randomly. Therefore, PM-FM transition transforms to PM-SG transition. Corresponding to the variation of the magnetic property, in the view of the electronic transport, the resistivity ρ increases and the temperature T_ρ shifts to low temperature with the doping content. For heavy doping, the samples exhibit an insulating behavior in the entire temperature range studied because of the strong localization of the p holes. Furthermore, the substitution of the Ti^{4+} ions extremely enhances the CMR effect in the perovskite manganite materials.

ACKNOWLEDGMENTS

The authors would like to thank Professor Lin Chen and Renyou Liang for help in experiments. This work was supported by the National Natural Science Foundation of China and The Research Fund for the Doctoral Program of Higher Education.

*Corresponding author. Email address: liuxm@ustc.edu.cn

[1] R. von Helmolt, J. Wecker, B. Holzapfel, L. Schultz, and K. Samwer, Phys. Rev. Lett. **71**, 2331 (1993).
[2] S. Jin, T. H. Tiefel, M. McCormack, R. A. Fastnacht, R. Ramesh, and L. H. Chen, Science **264**, 413 (1994).
[3] A. Urushibara, Y. Moritomo, T. Tomioka, A. Asamitsu, G. Kido, and Y. Tokura, Phys. Rev. B **51**, 14 103 (1995).
[4] A. P. Ramirez, J. Phys.: Condens. Matter **9**, 8171 (1997).
[5] C. Zener, Phys. Rev. **82**, 403 (1951).
[6] J. B. Goodenough, Phys. Rev. **100**, 564 (1955).
[7] R. Mahendiran, S. K. Tiwary, A. K. Raychaudhuri, T. V. Ramakrishnan, R. Mahesh, N. Rangavittal, and C. N. R. Rao, Phys. Rev. B **53**, 3348 (1996).
[8] A. J. Millis, P. B. Littlewood, and B. I. Shraiman, Phys. Rev. Lett. **74**, 5144 (1995).
[9] C. M. Varma, Phys. Rev. B **54**, 7328 (1996).
[10] J. L. Garcia-Munoz, M. Suaaidi, J. Fontcuberta, and J. Rodriguez-Carvajal, Phys. Rev. B **55**, 34 (1997).
[11] A. J. Millis, J. Appl. Phys. **81**, 5502 (1997).
[12] Naoto Nagaosa and Shuichi Murakami, Phys. Rev. B **57**, R6767 (1998).
[13] Young Sun, Xiaojun Xu, Lei Zheng, and Yuheng Zhang, Phys. Rev. B **60**, 12 317 (1999).
[14] G. J. Snyder, R. Hiskes, S. DiCarolis, M. R. Beasley, and T. H. Geballe, Phys. Rev. B **53**, 14 434 (1996).
[15] G. Jacob, W. Westerburg, F. Martin, and H. Adrian, Phys. Rev. B **58**, 14 966 (1998).
[16] K. H. Kim, J. Y. Gu, H. S. Choi, G. W. Park, and T. W. Noh, Phys. Rev. Lett. **77**, 1877 (1996).
[17] A. Shengelaya, Guo-meng Zhao, H. Keller, and K. A. Muller, Phys. Rev. Lett. **77**, 5296 (1996).
[18] S. J. L. Billinge, R. G. DiFrancesco, G. H. Kwei, J. J. Neumeier, and J. D. Thompson, Phys. Rev. Lett. **77**, 715 (1996).
[19] G. Zhao, K. Conder, H. Keller, and K. A. Muller, Nature (London) **381**, 676 (1996).
[20] Kebin Li, Xijun Li, Changsong Liu, Zhengang Zhu, Jiaju Du, Denglu Hou, Xiangfu Nie, Jingsheng Zhu, and Yuheng Zhang, Phys. Rev. B **56**, 13 662 (1997).
[21] H. L. Ju *et al.*, Phys. Rev. Lett. **79**, 3230 (1997).
[22] D. S. Dessau, T. Saitoh, C.-H. Park, Z.-X. Shen, P. Villella, N. Hamada, Y. Moritomo, and Y. Tokura, Phys. Rev. Lett. **81**, 192 (1998).
[23] M. F. Hundley *et al.*, Appl. Phys. Lett. **67**, 860 (1995).
[24] Y. Okimoto, T. Katsufuji, T. Ishikawa, T. Arima, and Y. Tokura, Phys. Rev. B **55**, 4206 (1997).
[25] K. H. Kim, J. H. Jung, and T. W. Noh, Phys. Rev. Lett. **81**, 1517 (1998).
[26] T. Saitoh, A. E. Bocquet, T. Mizokawa, H. Namatame, A.

Fujimori, M. Abbate, Y. Takeda, and M. Takano, Phys. Rev. B **51**, 13 942 (1995).
[27] A. S. Alexandrov and A. M. Bratkovsky, Phys. Rev. Lett. **82**, 141 (1999).
[28] C. Martin, A. Maignan, and B. Raveau, J. Mater. Chem. **6**, 1245 (1996).
[29] K. H. Ahn, X. W. Wu, K. Liu, and C. L. Chien, J. Appl. Phys. **81**, 5505 (1997).
[30] J. Blasco, J. Garcia, J. M. De Teresa, M. R. Ibarra, J. Perez, P. A. Algarabel, and C. Marquina, Phys. Rev. B **55**, 8905 (1997).
[31] C. Osthover, P. Grunberg, and R. R. Arons, J. Magn. Magn. Mater. **177-181**, 854 (1998).
[32] A. Maignan, C. Martin, and B. Raveau, Z. Phys. B: Condens. Matter **102**, 19 (1997).
[33] F. K. Lotgering, Philips Res. Rep. **25**, 8 (1970). In this paper, the LaBaMnTiO system was studied whose crystal structure was cubic. Our result is consistent with them.
[34] R. D. Shannon and C. T. Prewitt, Acta Crystallogr., Sect. A Cryst. Phys., Diffr., Theor. Gen. Crystallogr. **32**, 785 (1976).
[35] Lei Zheng, Kebin Li, and Yuheng Zhang, Phys. Rev. B **58**, 8613 (1998).
[36] F. K. Lotgering, Philips Res. Rep. **25**, 8 (1970).
[37] P. Schiffer, A. P. Ramirez, W. Bao, and S.-W. Cheong, Phys. Rev. Lett. **75**, 3336 (1995).